Remote Sensing of Environment 112 (2008) 3680–3689

Contents lists available at ScienceDirect

Remote Sensing of Environment

journal homepage: www.elsevier.com/locate/rse

Estimation of insect infestation dynamics using a temporal sequence of Landsat data

Nicholas R. Goodwin [a,*], Nicholas C. Coops [a], Michael A. Wulder [b], Steve Gillanders [a], Todd A. Schroeder [a], Trisalyn Nelson [c]

[a] Department of Forest Resource Management, 2424 Main Mall, University of British Columbia, Vancouver, Canada V6T 1Z4
[b] Canadian Forest Service (Pacific Forestry Center), Natural Resources Canada, 506 West Burnside Road, Victoria, Canada V8Z 1M5
[c] University of Victoria, Department of Geography, Victoria, Canada V8W 2Y2

ARTICLE INFO

Article history:
Received 6 December 2007
Received in revised form 20 May 2008
Accepted 24 May 2008

Keywords:
Mountain pine beetle
Landsat
Time series
Forest disturbance

ABSTRACT

The current outbreak of mountain pine beetle (*Dendroctonus ponderosae*) in western Canada has been increasing over the past decade and is currently estimated to be impacting 9.2 million hectares, with varying levels of severity. Large area insect monitoring is typically undertaken using manual aerial overview sketch mapping, whereby an interpreter depicts areas of homogenous insect attack conditions onto 1:250,000 or 1:100,000 scale maps. These surveys provide valuable strategic data for management at the provincial scale. The coarse spatial and attribute resolution of these data however, make them inappropriate for fine-scale monitoring and operational planning. For instance, it is not possible to estimate the initial timing of attack and year of stand death. In this study, we utilise eight Landsat scenes collected over a 14 year period in north-central British Columbia, Canada, where the infestation has gradually developed both spatially and temporally. After pre-processing and normalising the eight scenes using a relative normalisation procedure, decision tree analysis was applied to classify spectral trajectories of the Normalised Difference Moisture Index (NDMI). From the classified temporal sequence of images, key parameters were extracted including the presence of beetle disturbance and timing of stand decline. The accuracy of discriminating beetle attack from healthy forest stands was assessed both spatially and temporally using three years of aerial survey data (1996, 2003, and 2004) with results indicating overall classification accuracies varying between 71 and 86%. As expected, the earliest and least severe attack year (1996), recorded the lowest overall accuracy. The relationship between the timing of stand attack (*i.e.* moderate to severe beetle infestation) and NDMI (initial year of detected disturbance) was also explored. The results suggest that there is potential for deriving regional estimates of the year of stand death using Landsat data and decision tree analysis however, a higher temporal frequency of images is required to quantify the timing of mountain pine beetle attack.
© 2008 Elsevier Inc. All rights reserved.

1. Introduction

The current mountain pine beetle (*Dendroctonus ponderosae* Hopkins) infestation in western Canada is of previously unrecorded proportions impacting an estimated 9.2 million hectares in 2007 (Westfall, 2007). To minimise the economic impacts of the infestation on the forest industry and communities dependent on forestry operations, as well as reduce the ecological impacts of the infestation, it is important to identify the location and severity of beetle attack. Assessments of the current state of the forest resource are also needed for operational planning purposes, including the location of standing dead timber, year of beetle attack, and anticipated stand regeneration patterns.

The use of moderate-scale optical remote sensing imagery such as Landsat Thematic Mapper (TM) or Enhanced Thematic Mapper + (ETM+), with a spatial resolution of 30 m over a 185×185 km scene area, has been previously examined for its ability to discriminate spectral changes associated with beetle attack (Wulder et al., 2006a). When the intensity of mountain pine beetle attack is low, canopy cover declines gradually over time yielding subtle spectral changes which are often difficult to distinguish from healthy forests at various stages of succession (White et al., 2007). For example, Jakubauskas (1996) found that the spectral characteristics of beetle affected lodgepole pine (*Pinus contorta*) stands exhibit similar spectral responses as post-fire areas within Landsat imagery. The spectral separation of non-attack forest from stands with low intensity beetle attack was limited even with hyperspectral data from the Hyperion sensor (30 m resolution). This resulted in the recommendation that masking or stratifying regions of non-attack forest may be needed to minimise spectral variability unrelated to beetle attack (White et al., 2007). As directing image analysis to areas likely to contain beetle attack is expected to increase the disturbance map accuracy by reducing errors of commission (Rogan & Miller, 2007).

The examination of a temporal sequence of satellite images allows changes in reflectance associated with disturbance to be quantified and

* Corresponding author. Tel.: +1 604 822 6452; fax: +1 604 822 9106.
E-mail address: Nicholas.goodwin@ubc.ca (N.R. Goodwin).

0034-4257/$ – see front matter © 2008 Elsevier Inc. All rights reserved.
doi:10.1016/j.rse.2008.05.005

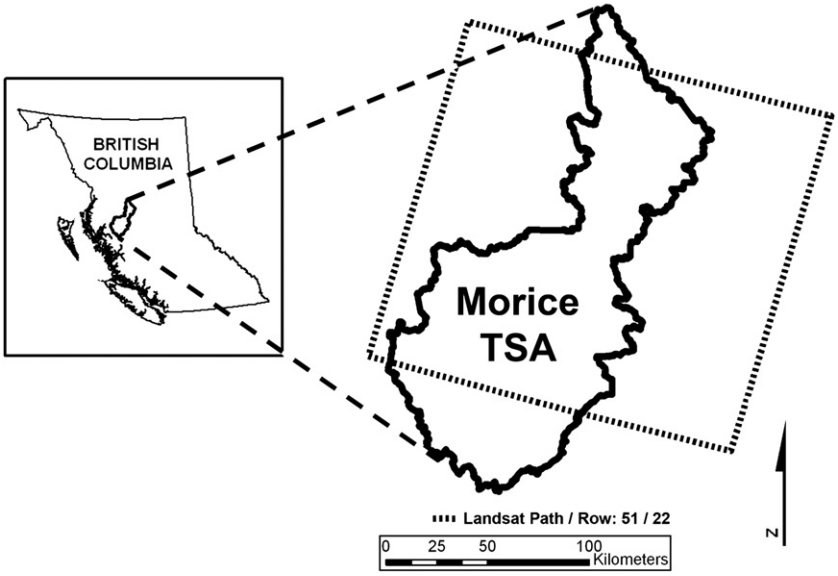

Fig. 1. Location of Morice timber supply area (TSA).

has been found to be effective at characterising disturbance events such as clear fell logging, selective logging, fire and insect outbreaks (Adams et al., 1995; Coppin et al., 2004; Coppin & Bauer, 1994; Fraser & Li, 2002; Kennedy et al., 2007; Roder et al., 2007; Wulder et al., 2005a). The key advantage of analysing multiple images, rather than a single image, is that a record of spectral reflectance change can be extracted to both characterise the magnitude and direction of physiological processes or disturbance events (Hostert et al., 2003) rather than seeking only the contrast between features of a single date of imagery. Change detection based on two image dates (surface reflectance or derived metric) have been used to characterise both the change direction and magnitude of a forest disturbance (Wulder et al., 2005a). For example, the Enhanced Wetness Disturbance Index (EWDI) has been widely used to characterise forest disturbance events (Franklin et al., 2001). This involves re-projecting the original Landsat (TM or ETM+) spectral bands along the principal directions of brightness, greenness, and wetness (known as a Tasseled Cap Transformation (TCT) (Crist & Cicone, 1984; Crist & Kauth, 1986; Kauth & Thomas, 1976) and then differencing the wetness band pre- and post-infestation (Skakun et al., 2003). To build upon these approaches, Wulder et al. (2006b) generated a probability surface of red attack damage from a logistic regression model that incorporated EWDI, elevation, and slope. Assuming a 50% threshold (>50% likelihood of attack=red attack), red attack damage was mapped with an accuracy of 83%. Similarly, Coops et al. (2006) derived estimates of beetle attack using a logistic regression model and two-date Landsat imagery. The results indicated that 70% of the beetle infestation sites were correctly classified with an independent set of beetle survey data used as validation.

The location of stand replacing disturbances (such as wildlife and clearcut logging) can be detected using a single set of before and after images, due to both their large visible extents and marked change in vegetation structure and function (Cohen et al., 2002). In contrast, subtle changes in forest condition such as foliage discolouration and defoliation due to insect attack, have proven more difficult to detect and map (Radeloff et al., 1999; Royle & Lathrop, 1997). However, the analysis of imagery from a number of years, rather than just two, may be more advantageous and accurate (Fisher et al., 2006; Hurley et al., 2004; Wilson & Sader, 2002), as an increased number of repeat observations will allow a temporal pattern to be developed allowing characterisation and interpretation of the reflectance patterns before, during, and after a given disturbance event. For example, the analysis of three Landsat images containing forest stands prior to disturbance, after insect defoliation (Gypsy moth, *Lymantria dispar*) and during refoliation, was found to improve the detection accuracy of infested areas, compared to two images (Hurley et al., 2004).

While studies examining temporal sequences of imagery have shown potential for increased accuracy in detecting non-stand replacing disturbances (Kennedy et al., 2007; Schroeder et al., 2007), a number of factors impact predictions of disturbance from spectral trajectories. In particular, gaps in the data record are a major limitation that can reduce the detection of phenology or disturbance events (Fisher et al., 2006; Franklin et al., 2005) resulting in errors of omission (Jin & Sader, 2005; Wilson & Sader, 2002). Large or frequent gaps in the image sequence will decrease the number of observations available to capture spectral trends and possibly affect their interpretation as fitted curves could misrepresent the true signal of a disturbance event. Furthermore, background conditions such as exposed soil or understorey vegetation (Radeloff et al., 1999) may increase the spectral variability of targeted disturbance events that occur in the overstorey canopy, making detection of changes more difficult. Confounding events based upon silvicultural treatments (such as herbicide application) can also produce unexpected changes to locations expected to be following a recovery trajectory (Franklin et al., 2005).

This study describes a new technique for classifying beetle attack based on a temporal sequence of Landsat data and a set of expert decision rules. The key components of this approach are that multiple images are considered in the classification of beetle attack and additional forest classes (*e.g.* harvesting or forest regrowth) can be integrated into the single classification. This approach was adopted over a trajectory based approach as it allows for low numbers of satellite images and data

Table 1
Field survey data characteristics

Attribute	Mean (SD)
Number of severely infested plots[a]	47
Average pine height (m)	26.32 (4.20)
Average pine diameter at breast height (m)	0.35 (0.08)
Number of green attack trees	225 (290)
Number of red attack trees	4 (9)
Number of grey attack trees	11 (17)

[a] >30 m away from non-forested locations (*e.g.* roads).

Table 2
Landsat TM image characteristics

Image acquisition date	Sensor
26th of June 1992	TM
3rd of October 1993	TM
24th of August 1996	TM
29th of July 1998	TM
14th of August 2001	ETM+
29th of September 2003	TM
14th of September 2004	TM
20th of August 2006	TM

gaps, which are a significant issue for mapping the mountain pine beetle in British Columbia due principally to cloud cover.

The objectives of this study are to:

1. Classify mountain pine beetle affected areas using a temporal sequence of pre- and post-beetle infestation Landsat images based on change thresholds, and
2. Explore the potential of using a temporal sequence of Landsat data to estimate key metrics of stand decline such as year of stand death, which is critical information for salvage harvesting, timber supply forecasting, and fire suppression.

2. Methods

2.1. Study area

The Morice Timber Supply Area (TSA) covers approximately 1.5 million hectares and is located in north north-central British Columbia, Canada (Fig. 1). Dominant tree species in the study area include lodgepole pine (*Pinus contorta*) and Spruce species (*Picea*), with pine accounting for approximately 50% of all species. Topography is characterised by steep mountains to the southwest and west, and is comparatively subdued to the north and east. The elevation range is between 500 and 2700 m. Five British Columbia Biogeoclimatic Ecological Classification (BEC) zones are reported within the Morice TSA that include: Sub-Boreal Spruce, Engelman Spruce–Subalpine Fir, Alpine Tundra, Coastal Western Hemlock, and Mountain Hemlock (British Columbia Ministry of Forests and Range, 1996). The Morice TSA represents the northern extent of the mountain pine beetle range and in this area populations are increasing. The variable timing of mountain pine beetle attack in this area makes it a suitable location to examine temporal trends of insect infestation. In the mid-1990's the primary mountain pine beetle infestation was located in the north and central region of the TSA which then expanded in the southern areas from 1999 onwards (Nelson et al., 2006a).

2.2. Mountain pine beetle overview

The mountain pine beetle life cycle typically involves beetles attacking and laying eggs in a host tree between mid-July to early August and, with exceptions based upon latitude and elevation, after ~1 year the next generation of beetles mature and emerge for flight, completing the life cycle. Infested trees are killed by two active processes: (1) mountain pine beetle infestation reduces the tree's defensive mechanism through "mass attack" and (2) fungal spores carried by the beetle disrupt the translocation of nutrients within the host tree. Tree mortality commonly occurs in late summer to early fall with needles remaining green for a short period of time (green attack stage), fading to yellow then red over the year after attack. Red needles (red attack stage) turn gray over time and are ultimately shed (gray attack stage) (Berryman, 1976; British Columbia Ministry of Forests and Range, 2007; Wulder et al., 2006a).

The mountain pine beetle infestation in the Morice region has been widespread. In the mid-1990s the small pockets of intense infestation in the north were heavily managed. Infestation rates were similar in the mid-portion of the study area, but management was less intense. In the south the infestation was delayed until 1999 or 2000, after which it was very intense and management was not considered an option. For tactical planning purposes, forest managers have utilised helicopter

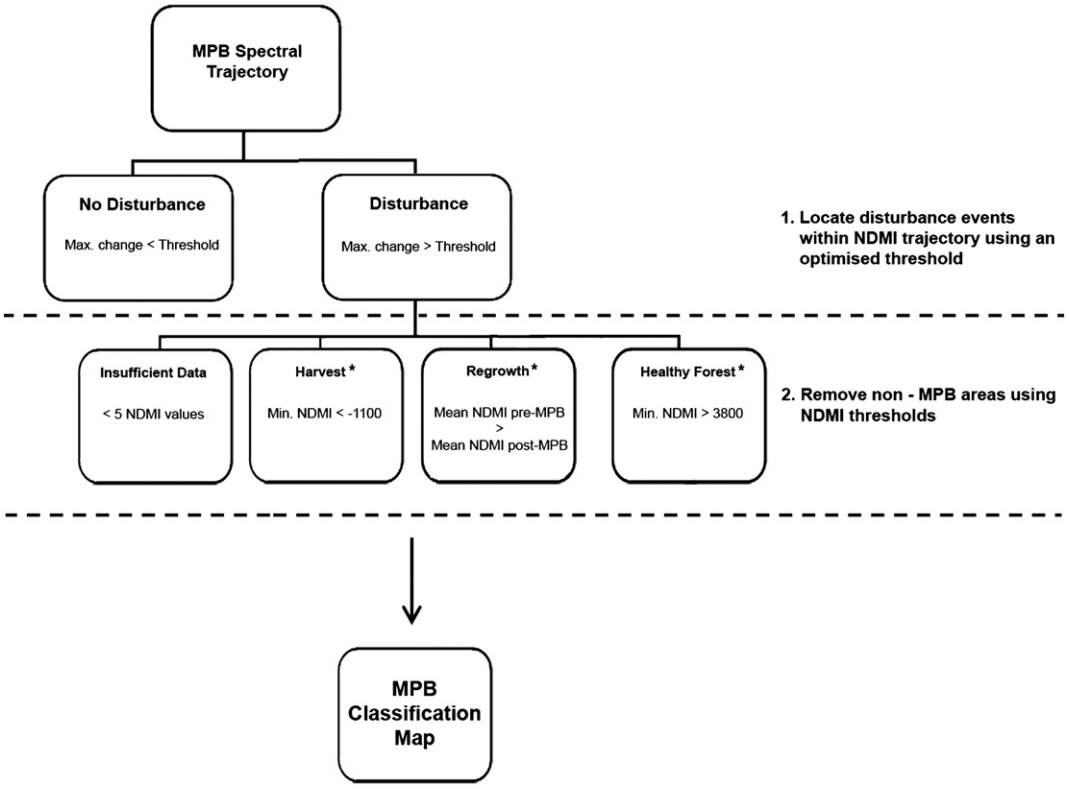

Fig. 2. Characteristics of the decision tree classifier. **Note*: class labels are applied based upon visual interpretation.

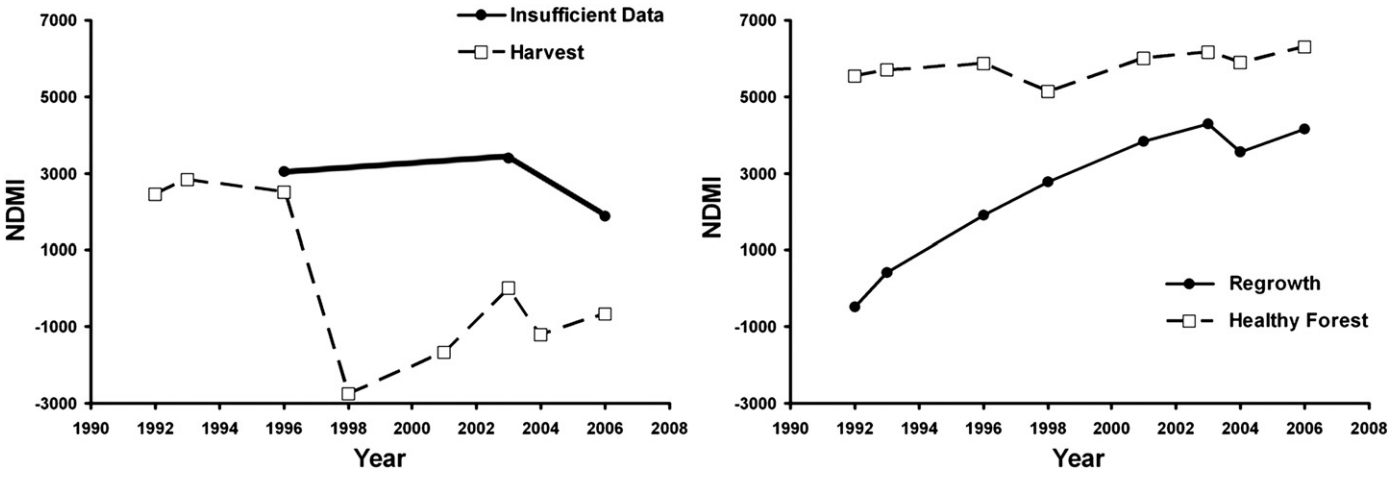

Fig. 3. Non-MPB disturbance examples detected by the decision tree classifier.

surveys to assess the impact and location of the mountain pine beetle outbreak. Helicopter based aerial observations of red attack damage have been undertaken annually over the entire TSA and involves trained observers locating forest stands with red attack trees and recording a GPS location along with an estimate of the number of damaged trees in three classes: red attack (trees with red crowns), gray attack (dead trees with no needles), and yellow/green (trees changing colour from green to red; known as "faders"). The maximum area for each helicopter sample point is equal to 0.031 km^2 or a circular area with a 100 m radius (Nelson et al., 2006b). Approximately 93% of locations have attributes accurate within ±10 trees and spatial error estimated at ±25 m (Nelson et al., 2006a).

In addition to the helicopter surveyed locations of mountain pine beetle red attack, field plot data were available detailing mountain pine beetle attack in Morice TSA. The field plots were established as a series of circular plots with a radius of 8 m (total area = 200 m^2 or 1/50th of a hectare). At each plot forest structural attributes such as maximum tree height and stem diameter were measured along with an assessment of the mountain pine beetle impact for two years (2003 to 2004). These mountain pine beetle measurements include the number of trees currently attacked, the number of trees attacked 1 and 2 years previously (*i.e.* red or gray attack), as well as an estimate of the total area of infestation (*refer* Table 1 for details).

Furthermore, aerial observation data has been transformed to develop a province province-wide severity map at a spatial resolution of 1 ha (Wulder et al., in review). The transformation involved populating each pixel with a severity code (1 to 5, ranging from trace to severe mountain pine beetle attack) for the intersecting year of aerial survey data. The result is an annual, province-wide, 1 ha layer of beetle severity (either 3 or 5 class code) and extent from 2000 to 2005.

2.3. Landsat data and pre-processing

Seven Landsat-5 TM and one Landsat-7 Enhanced Thematic Mapper (ETM+) scenes were acquired between 1992 and 2006 to characterise the mountain pine beetle outbreak over the Morice TSA (Path/Row: 51/22; Table 2). These images were all captured within the summer/fall seasonal window to maximise the amount of red attack damage and related changes in spectral reflectance. Extensive cloud cover prevented the use of annual dates of imagery; no gap in the image dates exceeded 3 years but cloud cover within scenes further contributed to data gaps.

Data pre-processing involved two critical steps. First image-to-image geometric registration was undertaken using a nearest-neighbour 2nd order polynomial transformation to minimise any geometric offsets or distortions within the image stack. The 2001 ortho-rectified image was used as the base image (Table 2) due to its lack of cloud cover. All other images were rectified with a root mean square error < 0.5 pixels or 15 m. Areas of cloud and cloud shadow were removed via manual interpretation.

As variations due to different atmospheric conditions, solar angle, and sensor characteristics are likely to limit the ability to characterise spectral change due to mountain pine beetle attack (Chen et al., 2005), the second

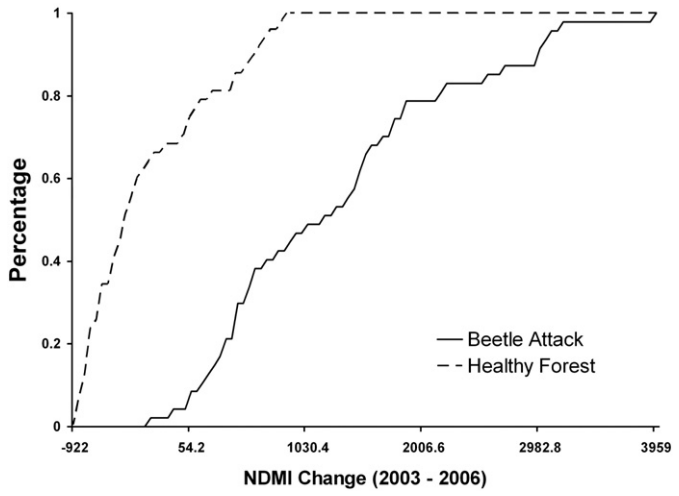

Fig. 4. Cumulative histograms of NDMI change (relative to pre-infestation, 2003 to 2006) plotted as a percentage of the total observations.

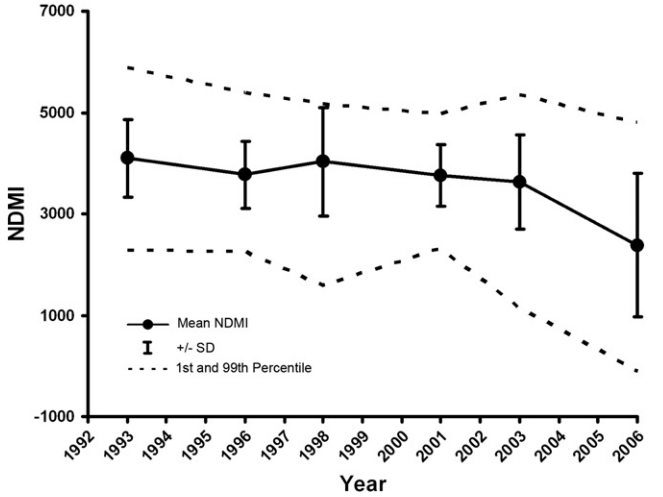

Fig. 5. Mean NDMI profile for field surveyed MPB plots. *Note*: the 2004 data was excluded from this figure due to cloud cover limiting the number of plots.

critical step involved the radiometric normalisation of images to ensure that changes in spectral reflectance between years correspond to meaningful physiological events. To do this we first atmospherically corrected the 2001 base image to estimate surface reflectance using the COST model (corrects for cosine of the solar zenith angle) (Chavez, 1996). Next we applied the Multivariate Alteration Detection (MAD) algorithm (Canty et al., 2004; Schroeder et al., 2006) which utilises canonical correlation analysis to locate invariant pixels for use in matching the remaining images to our atmospherically corrected base image. MAD has the advantage of being an automated approach, has been demonstrated to work well in forested environments, and when used in this context corrects all images of atmospheric effects during the simultaneous conversion to units of surface reflectance (Schroeder et al., 2006). Our implementation of the MAD algorithm followed that of Schroeder et al. (2006), differing only through our use of four 1000×1000 pixel image subsets (instead of one) to locate invariant pixels. Using additional image subsets will ensure that the full range of spectral variation is sampled, as a single subset may not cover a sufficient range of cover types. The invariant pixels located within each of the image subsets were used to develop band-wise regression equations for relative normalisation.

Following data pre-processing, the Normalised Difference Moisture Index (NDMI) was calculated using Eq. (1) and converted to integer format (multiplied by 10,000) for each image. NDMI contrasts a near-infrared (NIR) spectral band, which is sensitive to changes in the number and configuration of air spaces that form the internal leaf structure (Sinclair et al., 1971), with a mid-infrared (MIR) spectral

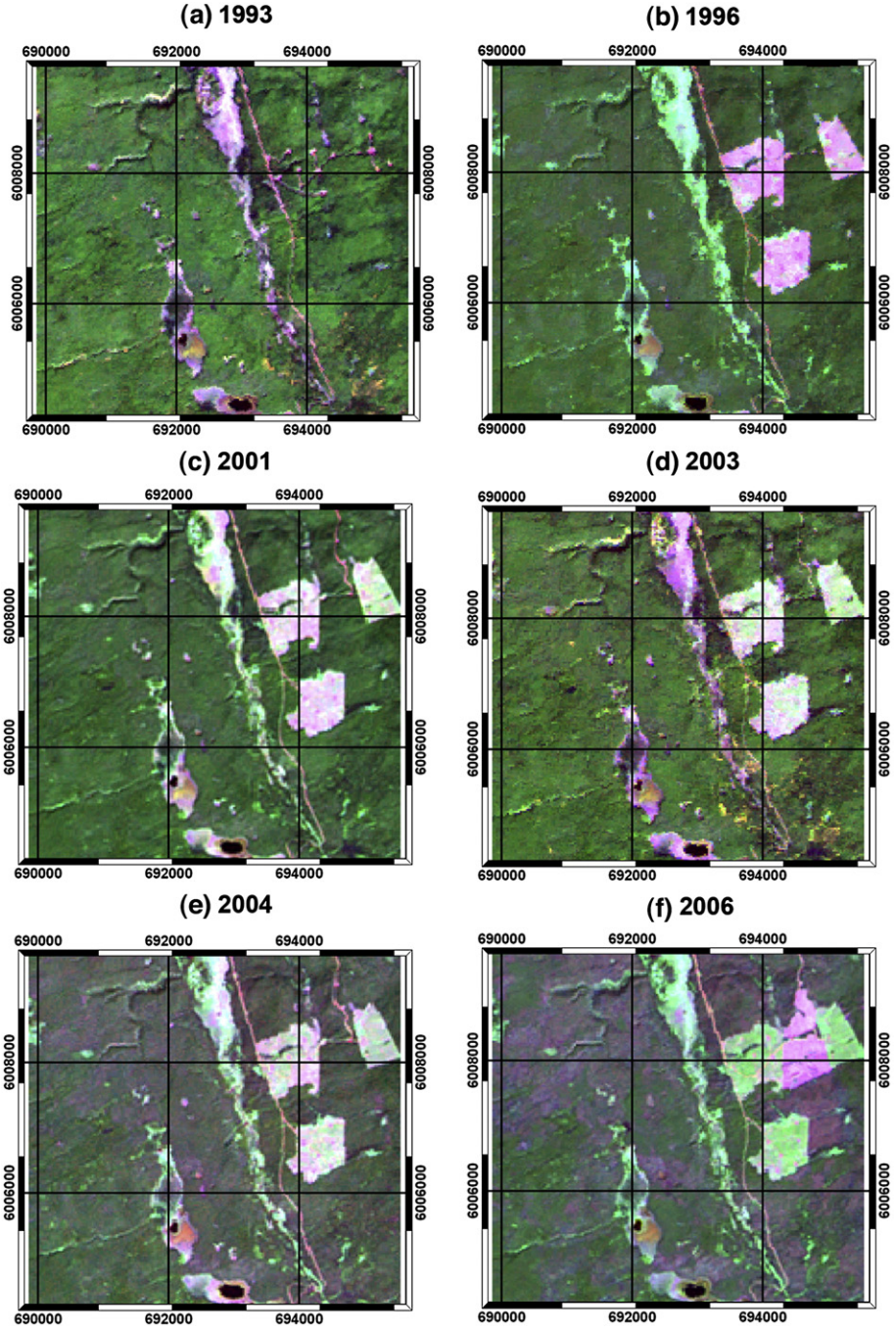

Fig. 6. Image subset of Morice TSA displaying MPB attack between 1993 and 2006. *Note*: the RGB band combination used was Landsat TM bands 5, 4, and 3 with a 2 SD stretch. Dark green areas represent healthy forest, reddish areas MPB, and harvested areas light green or magenta.

Table 3
Classification results for 1996 aerial survey data (max. change between 1993 and 1998)

	Aerial survey data		Total
	Mountain pine beetle attack	No red attack	
Classification			
Mountain pine beetle attack	140	17	157
No red attack	147	270	417
Total	287	287	574

Mountain pine beetle attack producer's accuracy=49% (+/−5% at the 90% confidence interval).
No red attack producer's accuracy=94% (+/−2% at the 90% confidence interval).

Table 5
Classification results for 2004 aerial survey data (max. change between 2003 and 2006)

	Aerial survey data		Total
	Mountain pine beetle attack	No red attack	
Classification			
Mountain pine beetle attack	1460	115	1575
No red attack	394	1739	2133
Total	1854	1854	3708

Mountain pine beetle attack producer's accuracy=79% (+/−2% at the 90% confidence interval).
No red attack producer's accuracy=94% (+/−1% at the 90% confidence interval).

band where absorbance is principally governed by the vegetation water content (Curran, 1989; Kumar et al., 2006).

$$\mathrm{NDMI} = \frac{\mathrm{TM\ band\ 4\ (NIR)} - \mathrm{TM\ band\ 5\ (MIR)}}{\mathrm{TM\ band\ 4\ (NIR)} + \mathrm{TM\ band\ 5\ (MIR)}} \quad (1)$$

This metric was chosen due to its proven sensitivity to quantify forest disturbance events (Jin & Sader, 2005; Wilson & Sader, 2002), and has been shown to be highly correlated with the TCT wetness metric in earlier studies (Jin & Sader, 2005). Given that geometric registration errors greater than 1 pixel may exist within the dataset, as discussed by Kennedy et al. (2007), a low pass filter (3×3 pixels) was applied to the NDMI images to minimise the impact caused by any mis-registration.

2.4. Classification of mountain pine beetle infested areas

In order to classify NDMI changes through time we applied an expert decision tree approach, which splits the dependent variable (in this case NDMI) using optimal threshold values. A decision tree can be considered as a sequence of binary nodes (yes/no queries) dividing a dependent variable into homogeneous subsets of response values depending on whether it fulfills a given condition. Each node can either lead to another node or to a fitted response value, corresponding to a labelled predictor variable (terminal node). This type of modelling approach, based on either statistical data mining approaches or a series of expert rules, is becoming more widespread in ecological research (De'ath & Fabricius, 2000; Lucas et al., 2007; Schwalm et al., 2006) as it is flexible and easily encapsulates meaningful trends in the data (Melendez et al., 2006; Schwalm et al., 2006).

The derivation of the disturbance threshold involved extracting the NDMI values at each of the 47 field plots sampled in 2004. All field plots had evidence of moderate to high levels of attack (>25% red attack area per plot) between 2003 and 2006 and were further than 30 m from a road or harvest disturbance. In addition, we extracted the NDMI values for a commensurate number of healthy plots greater than 30 m from roads with no evidence of red attack. As healthy areas were not recorded in aerial surveys, we developed a proxy measure based on the Normalised Difference Vegetation Index (NDVI) (*sensu* Coops et al., 2006; Wulder et al., 2005a). The assumption with using NDVI as a proxy measure is that beetle attacked locations will not have high levels of photosynthetic activity. This involved computing NDVI for the 2006 image (last image of the dataset) and randomly selecting locations with a high NDVI (>0.85).

Upon examination of all of spectral trajectories it was apparent that a number of key trends existed. First, despite large variation in the magnitude of the NMDI, in cases where mountain pine beetle was observed, the NDMI value fell relative to the pre-infestation value. Conversely, if the stand condition was not infested the NMDI showed no significant decline relative to the initial pre-infestation value and increased over time when the pixels covered a regrowth stand. In situations where a stand was clear felled and bare soil remained, the NDMI value fell immediately to values less than that of any other vegetation in the scene, regardless of stand condition.

Based on these observations of NDMI behaviour, five key thresholds and rules were defined. The rules were then optimised by visually comparing classification results with Landsat imagery and surveyed locations of beetle attack (Figs. 2 and 3). The five rules include:

1. Forest re-growth: NDMI value increases over time period
2. Harvest event: NDMI value falls below a preset value
3. Healthy forest: NDMI remains above a preset value
4. Mountain pine beetle infestation: NDMI falls by threshold value but not greater than the predefined harvesting value
5. No disturbance: Situations where less than 5 out of the 8 pixels values contained spectral values (*i.e.* cloud or shadow present in greater than 3 images) or the change in NDMI magnitude is less than the predefined beetle attack threshold.

To assess the magnitude of the mountain pine beetle change threshold relative to the pre-infestation levels and non-attack forest, a set of known red attack field plots and non-attack locations were examined. The change in NDMI between 2003 and 2006 was then calculated, and used to develop two cumulative histograms of NDMI change for beetle attack and non-attack areas. Based on these cumulative histograms, an optimal threshold was defined which corresponds to the value where

Table 4
Classification results for 2003 aerial survey data (max. change between 2001 and 2006)

	Aerial survey data		Total
	Mountain pine beetle attack	No red attack	
Classification			
Mountain pine beetle attack	101	10	126
No red attack	28	119	132
Total	129	129	258

Mountain pine beetle attack producer's accuracy=78% (+/−6% at the 90% confidence interval).
No red attack producer's accuracy=92% (+/−4% at the 90% confidence interval).

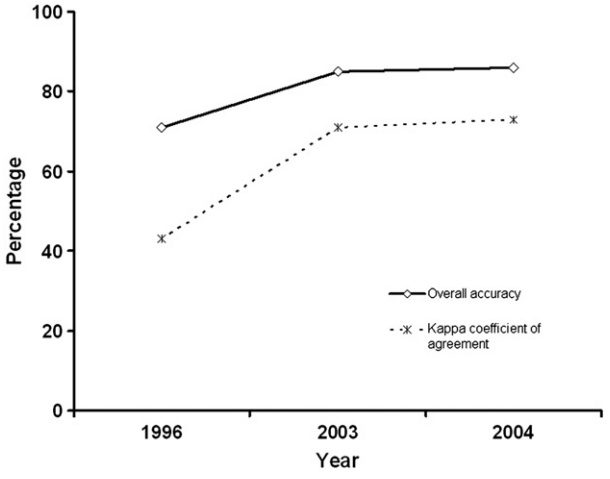

Fig. 7. Classification accuracy results.

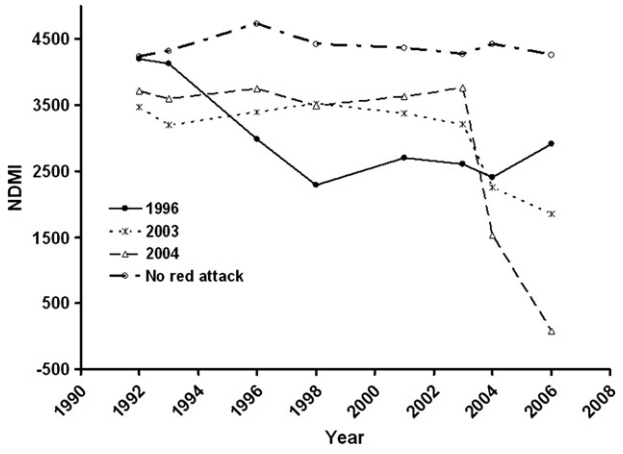

Fig. 8. Spectral trajectory curves derived from validation plots. *Note*: each curve is derived from one pixel location to illustrate the different types of response.

commission and omission errors are minimised. In addition, we identified the timing of stand decline from the temporal sequence of Landsat images by extracting the first year which exceeds the change threshold. All pixels flagged as the initial year of disturbance were summed to derive regional estimates of the area killed by year. Given that NDMI continues to decline for a number of years following beetle attack, the year of minimum NDMI was not linked to the timing of stand decline.

2.5. Evaluation

The accuracy of the decision tree threshold values were evaluated using the independent helicopter based survey data collected in 1996, 2003, and 2004. The accuracy assessment included both an evaluation of the beetle attack classification accuracy as well as the timing of attack. Confidence interval estimates were also calculated using sample size and accuracy percentage data to indicate the certainty of the results relative to the true population (Czaplewski, 2003; Wulder et al., 2005b). The three years of helicopter surveyed locations were individually overlaid on the output of the decision rules, and the classification code from the set of decision rules extracted. Similarly, the locations of stands without red attack as estimated from the 2006 imagery were overlaid and the codes extracted and compared. As the focus of the paper is on the capture of mountain pine beetle infestation (and mapping accuracy), pixels classified as healthy or regrowth forest were combined, and the areas with less than 5 observed NMDI values removed.

3. Results

The cumulative histograms of NDMI change computed as the difference between pre- and post-beetle infestation for the forest plots are shown in Fig. 4. This figure shows that the beetle infested and forest pixels without red attack (*i.e.* healthy) are largely separable based on magnitudes of change that range from −900 to 4000. At lower threshold values (<1000) however, there is an overlap in the range of values in the

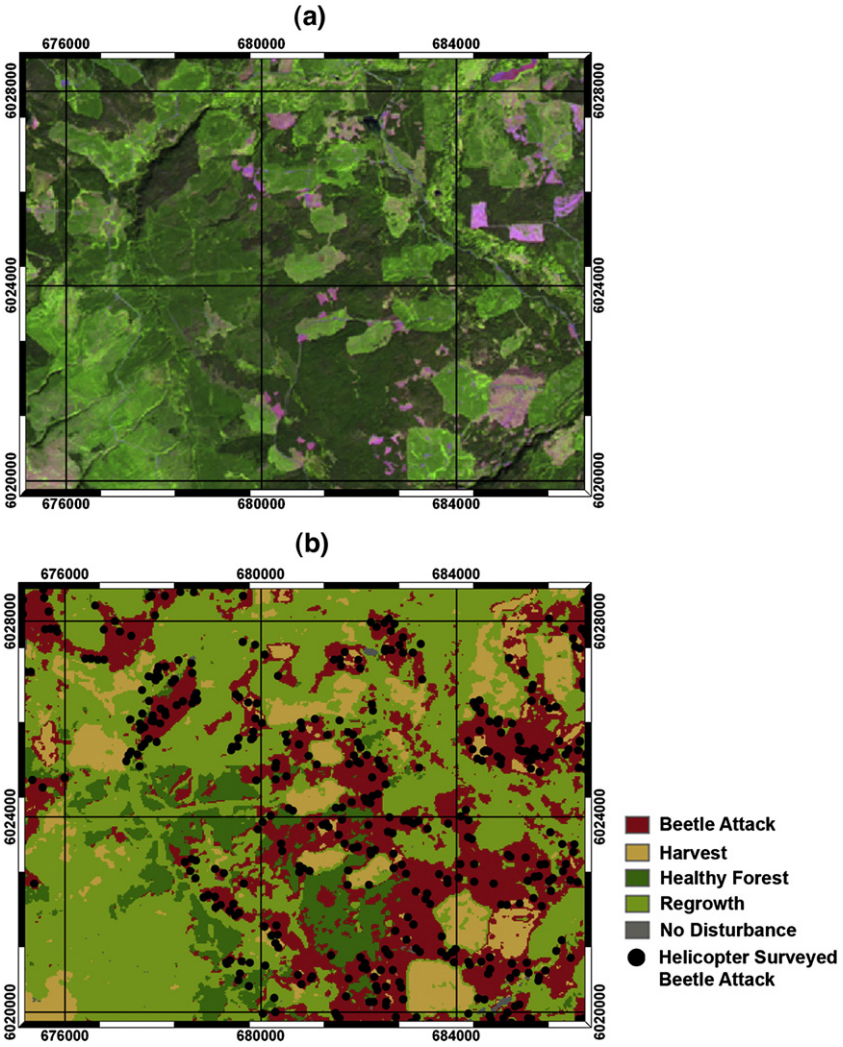

Fig. 9. Classified map result: (a) 2006 Landsat image (RGB, bands 5,4,3) and (b) classified map with helicopter-GPS locations surveyed in 2004.

two cumulative histograms indicating that the mountain pine beetle locations characterised by a subtle change in NDMI may be difficult to discriminate from non-attacked forest. Based on these results, an optimum threshold value was set at the point which minimised both commission and omission errors (*i.e.* NDMI change >590). Using this threshold, it can be expected that ~75% of mountain pine beetle attacked areas will be correctly classified (Fig. 4), while approximately 5% of mountain pine beetle infested sites experienced an increase in NDMI relative to pre-infestation levels.

The general NDMI characteristics of the 47 field plots infested with mountain pine beetles are shown in Fig. 5. The mean NDMI trajectory for all plots (regardless of year of infestation) reveals that from 1992 to 2003 only minor variation occurs in NDMI values (differences<590) which is expected due to the low amount of infestation in the early part of the time sequence. After 2003 however, the overall trajectory declines which is consistent with the wide spread infestation observed between 2004 and 2006 (Fig. 6). The standard deviation (and extremes) of the NDMI trajectory for the field plots also confirms that significant variation exists in healthy forest stands, before the outbreak in 2003. Prior to infestation in 1993, for example, there is 50% variation around the mean simply due to natural variation. However, over time there is a decreasing trend in the mean and the extremes of the data, which is indicative of increasing levels of infestation. Additional examination of the data also confirmed that low levels of infestation produced smaller changes in NDMI compared to the comparatively large decreases in NDMI observed for more heavily attacked stands.

The accuracy of the decision tree classification was evaluated using three years of helicopter survey data (1996, 2003, and 2004; Table 3–5) and indicates overall classification accuracies of 71, 84 and 86% respectively (Kappa accuracy ranging from 43 to 73%; Fig. 7). The no red attack forest class recorded the highest classification accuracies for all years (producer's accuracy ranging from 92 to 94%) while the beetle attack class accuracies were poorer. Given the potential for variable rates of discolouration due to climate and stand condition, the lower accuracy of classifying mountain pine beetle attack compared to healthy forest is expected and consistent with earlier research classifying foliage discolouration (Radeloff et al., 1999). In 1996 the ability to classify mountain pine beetle was limited with 49% of pixels correctly classified (producer's accuracy, +/−5% at the 90% confidence interval). However, in 2003 and 2004 the producer's accuracy increased to 78 and 79%, respectively. The lower accuracy recorded in 1996 is most likely due to the lower severity of mountain pine beetle attack as this year is at the leading edge of the infestation which has been demonstrated to result in lower classification accuracies (Skakun et al., 2003). The NDMI trajectories in Fig. 8 are also able to illustrate the NDMI decline characteristics between years, which in most cases were larger for mountain pine beetle surveyed areas in 2003 and 2004 relative to 1996. The variation in NDMI for areas characterised with no red attack indicates no decrease over time greater than the threshold value of 590.

To provide additional confidence that the derived classes are spatially meaningful, a Landsat image and corresponding classification map with helicopter-GPS survey locations is shown in Fig. 9. Importantly, this shows good agreement between the surveyed locations and classified beetle attack areas. Also the harvest and regrowth forest areas appear to be well characterised.

The initial year of disturbance (*i.e.* the first year a NDMI change exceeds the threshold) as a percentage of total mountain pine beetle area, is shown in Fig. 10a. This shows a general increasing trend from 1993 to 2006, with the 2006 year recording the largest percentage of initial disturbance (9%). Likewise the percentage of mountain pine beetle area with moderate to high levels of attack, according to the aerial survey disturbance map, reveals an increase in mountain pine beetle area over time and the highest percentage occurring in 2005 (14%; Fig. 10b). However, it should be noted that these results are not directly comparable due to different years of assessment caused by gaps in the Landsat dataset.

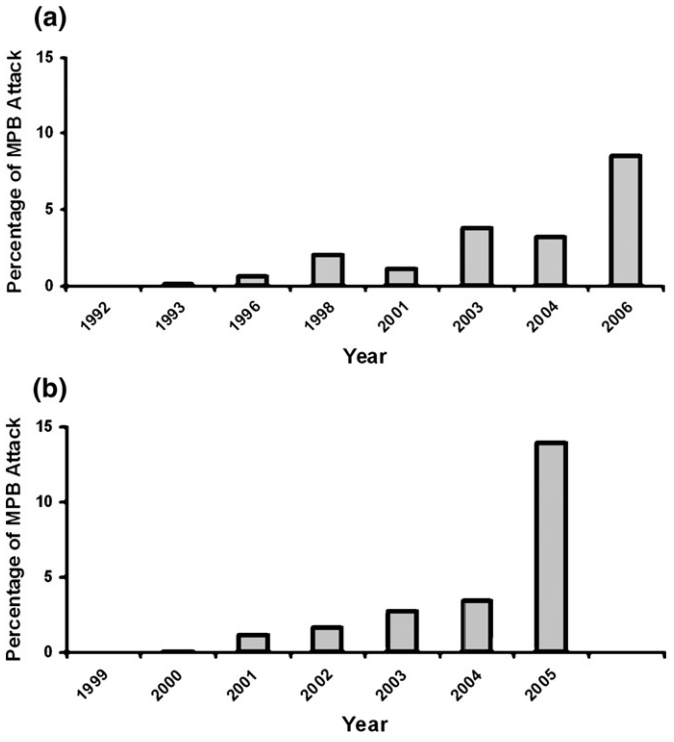

Fig. 10. Regional assessment of MPB disturbance at the Landsat scene scale: (a) initial year of disturbance derived from NDMI data, and (b) gridded aerial survey data. *Note*: the number of MPB detected pixels between years were normalised to account for differences in the number of pixels containing data.

Overall, the final classification found that 17% or 4500 of the 26,478 km^2 of the classified Landsat TM scene area was affected by the mountain pine beetle between 1992 and 2006. This is likely to be an underestimate of the true mountain pine beetle area due to salvage harvest operations targeting mountain pine beetle infested areas within the Morice TSA.

4. Discussion

In this study we applied a threshold based decision tree approach to a large number of spectral trajectories to classify the presence of mountain pine beetle infestation, as well as characterise post-attack stand condition. Our findings show that changes in NDMI due to mountain pine beetle infestation were generally larger than that of a healthy forest (*i.e.* no red attack); however, it is evident that some spectral confusion exists, especially for forest stands with low levels of infestation. For example, the 1996 aerial survey locations had a lower accuracy relative to the 2003 and 2004 surveys. This result is consistent with other research which demonstrates that stands with 10–29 red attack trees were more difficult to classify than sites with 30 to 50 red attack trees using the EWDI over a two year period (1999 to 2001) (Skakun et al., 2003). Furthermore, greater declines in NDMI values were evident following mountain pine beetle attack in 2003 and 2004 (Fig. 8), which increased the number of plots exceeding the disturbance threshold and thus the classification accuracy.

Data gaps within the temporal sequence of imagery were a significant issue in this research, which prevented yearly monitoring of NDMI change across the landscape. Typically, trees infested with the mountain pine beetle die in year 1 (green attack), turn red in year 2 and then gray in years 3 to 5. Consequently, the accurate capture of NDMI trends will require yearly observations. If a higher temporal frequency of images were available, we anticipate that trajectory based techniques (*e.g.*

Kennedy et al., 2007) could improve the accuracy of beetle attack classifications and eliminate the need for re-training of thresholds when applied to other areas. The ability to reference the natural variability of NDMI pre-infestation, for example, could allow subtle beetle related trends that are less than the disturbance threshold to be detected. Likewise, approaches which classify imagery into a set of classes and subsequently, examine the order of classes (Zhou et al., 2008) may be beneficial for examining beetle attack dynamics. If applied operationally, an additional limitation with approaches based on decision rules rather than trajectories is the need to re-train these rules for different geographic areas.

Despite these difficulties we believe there are a number of key advantages with using an approach based on decision rules to assess insect infestation dynamics. These include the capacity to integrate our knowledge of the physiological behaviour of mountain pine beetle infested forest stands with the behaviour of NDMI over time and to assess the cumulative area of mountain pine beetle attack over a number of years using a single classification process. There are however, a number of factors that make it difficult to consistently locate mountain pine beetle infestation at the landscape scale. The most critical of these, other than difficulties in detecting low rates of infestation, is the added complexity of salvage logging operations that are occurring in the region due to the infestation. This highly dynamic landscape makes establishing long term sites without additional disturbance a difficult task.

This study also indicated a relationship between the timing of stand decline and NDMI computed with multiyear Landsat data. Importantly, it was found that the area estimates of annual mountain pine beetle attack derived from the sequences of NDMI data (*i.e.* initial year of disturbance) were comparable to the estimates based on gridded aerial survey data at the regional scale, providing additional confidence in the proposed approach. For example, an increase in the area of mountain pine beetle attack from the late 1990s onwards, with the largest increase occurring after 2004, was evident in both datasets. This suggests a regional assessment of mountain pine beetle attack over time, with accuracies comparable to aerial survey data, might be possible using an approach based on decision rules and Landsat imagery.

5. Conclusions

Multiyear datasets derived from moderate resolution data from sensors such as Landsat provide a valuable source of information for characterising disturbance events such as the mountain pine beetle outbreak in British Columbia. Using a series of pre- and post post-infestation images, we found that mountain pine beetle infestation locations can be classified at a moderate to high level of accuracy; levels of accuracy useful for some forest management and operational planning activities. The use of a decision threshold for beetle attack was found to be effective (*i.e.* accuracies>70% for 2003 and 2004) as large changes in NDMI exceeding the disturbance threshold frequently occurred between image dates at surveyed beetle attack locations. The relationship between the timing of stand decline and NDMI was also investigated with the initial year of disturbance providing positive results. This suggests that the analysis of a temporal sequence of Landsat images may be suitable for characterising the year of death for a given pixel. Additional image dates leading to a higher temporal frequency however, are needed to better quantify the spectral response due to beetle attack.

Acknowledgements

This project is funded by the Government of Canada through the Mountain Pine Beetle Initiative, a six-year, $40 million program administered by Natural Resources Canada, Canadian Forest Service. Additional information on the Mountain Pine Beetle Initiative may be found at: http://mpb.cfs.nrcan.gc.ca. Some of the Landsat data used in this study was contributed by the U.S. Geological Survey Landsat Data Continuity Mission Project through participation of MAW on the Landsat Science Team.

References

Adams, J. B., Sabol, D. E., Kapos, V., Almeida, R., Roberts, D. A., Smith, M. O., & Gillespie, A. R. (1995). Classification of multispectral images based on fractions of endmembers — Application to land-cover change in the Brazilian Amazon. *Remote Sensing of Environment*, *52*(2), 137–154.

Berryman, A. A. (1976). Theoretical explanation of mountain pine beetle dynamics in Lodgepole pine forests. *Environmental Entomology*, *5*(6), 1225–1233.

British Columbia Ministry of Forests a (1996). *Morice TSA timber supply analysis. In: Province of British Columbia Ministry of Forests.*

British Columbia Ministry of Forests a (2007). *Timber supply and the mountain pine beetle infestation in British Columbia: 2007*. update. In (p. 38). Canada: http://www.for.gov.bc.ca/hfp/mountain_pine_beetle/Pine_Beetle_Update20070917.pdf

Canty, M. J., Nielsen, A. A., & Schmidt, M. (2004). Automatic radiometric normalization of multitemporal satellite imagery. *Remote Sensing of Environment*, *91*(3–4), 441–451.

Chavez, P. S. (1996). Image-based atmospheric corrections — Revisited and improved. *Photogrammetric Engineering and Remote Sensing*, *62*(9), 1025–1036.

Chen, X., Vierling, L., & Deering, D. (2005). A simple and effective radiometric correction method to improve landscape change detection across sensors and across time. *Remote Sensing of Environment*, *98*(1), 63–79.

Cohen, W. B., Spies, T. A., Alig, R. J., Oetter, D. R., Maiersperger, T. K., & Fiorella, M. (2002). Characterizing 23 years (1972–95) of stand replacement disturbance in western Oregon forests with Landsat imagery. *Ecosystems*, *5*(2), 122–137.

Coops, N. C., Johnson, M., Wulder, M. A., & White, J. C. (2006). Assessment of QuickBird high spatial resolution imagery to detect red attack damage due to mountain pine beetle infestation. *Remote Sensing of Environment*, *103*(1), 67–80.

Coppin, P., Jonckheere, I., Nackaerts, K., Muys, B., & Lambin, E. (2004). Digital change detection methods in ecosystem monitoring: A review. *International Journal of Remote Sensing*, *25*(9), 1565–1596.

Coppin, P. R., & Bauer, M. E. (1994). Processing of multitemporal Landsat TM imagery to optimize extraction of forest cover change features. *IEEE Transactions on Geoscience and Remote Sensing*, *32*(4), 918–927.

Crist, E. P., & Cicone, R. C. (1984). Application of the tasseled cap concept to simulated Thematic Mapper data. *Photogrammetric Engineering and Remote Sensing*, *50*(3), 343–352.

Crist, E. P., & Kauth, R. J. (1986). The tasseled cap de-mystified. *Photogrammetric Engineering and Remote Sensing*, *52*(1), 81–86.

Curran, P. J. (1989). Remote sensing of foliar chemistry. *Remote Sensing of Environment*, *30*(3), 271–278.

Czaplewski, R. L. (2003). Accuracy assessment of maps of forest condition: Statistical design and methodological considerations. In M. A. Wulder, & S. E. Franklin (Eds.), *Remote sensing of forest environments: Concepts and case studies* (pp. 115–140). Boston, Mass: Kluwer Academic Publishers.

De'ath, G., & Fabricius, K. E. (2000). Classification and regression trees: A powerful yet simple technique for ecological data analysis. *Ecology*, *81*(11), 3178–3192.

Fisher, J. I., Mustard, J. F., V, & adeboncoeur, M. A. (2006). Green leaf phenology at Landsat resolution: Scaling from the field to the satellite. *Remote Sensing of Environment*, *100*(2), 265–279.

Franklin, S. E., Jagielko, C. B., & Lavigne, M. B. (2005). Sensitivity of the Landsat enhanced wetness difference index (EWDI) to temporal resolution. *Canadian Journal of Remote Sensing*, *31*(2), 149–152.

Franklin, S. E., Lavigne, M. B., Moskal, L. M., Wulder, M. A., & McCaffrey, T. M. (2001). Interpretation of forest harvest conditions in New Brunswick using Landsat TM enhanced wetness difference imagery (EWDI). *Canadian Journal of Remote Sensing*, *27*(2), 118–128.

Fraser, R. H., & Li, Z. (2002). Estimating fire-related parameters in boreal forest using SPOT VEGETATION. *Remote Sensing of Environment*, *82*(1), 95–110.

Hostert, P., Roder, A., & Hill, J. (2003). Coupling spectral unmixing and trend analysis for monitoring of long-term vegetation dynamics in Mediterranean rangelands. *Remote Sensing of Environment*, *87*(2–3), 183–197.

Hurley, A., Watts, D., Burke, B., & Richards, C. (2004). Identifying gypsy moth defoliation in Ohio using Landsat data. *Environmental & Engineering Geoscience*, *10*(4), 321–328.

Jakubauskas, M. E. (1996). Thematic Mapper characterization of lodgepole pine seral stages in Yellowstone National Park, USA. *Remote Sensing of Environment*, *56*(2), 118–132.

Jin, S. M., & Sader, S. A. (2005). Comparison of time series tasseled cap wetness and the normalized difference moisture index in detecting forest disturbances. *Remote Sensing of Environment*, *94*(3), 364–372.

Kauth, R. J., & Thomas, G. S. (1976). *The tasseled cap—A graphic description of spectral–temporal development of agricultural crops as seen by Landsat.* Final Proceedings: 2nd International Symposium on Machine Processing of Remotely Sensed Data. West Lafayette, Purdue University.

Kennedy, R. E., Cohen, W. B., & Schroeder, T. A. (2007). Trajectory-based change detection for automated characterization of forest disturbance dynamics. *Remote Sensing of Environment*, *110*(3), 370–386.

Kumar, L., Schmidt, K., Dury, S., & Skidmore, A. (2006). Imaging spectrometry in vegetation science. In F. D. Meer, & S. M. de Jong (Eds.), *Imaging Spectroscopy: Basic principles and prospective applications* (pp. 111–155). Dordrecht: Springer Publishers.

Lucas, R., Rowlands, A., Brown, A., Keyworth, S., & Bunting, P. (2007). Rule-based classification of multi-temporal satellite imagery for habitat and agricultural land cover mapping. *ISPRS Journal of Photogrammetry and Remote Sensing*, *62*(3), 165–185.

Melendez, K. V., Jones, D. L., & Feng, A. S. (2006). Classification of communication signals of the little brown bat. *Journal of the Acoustical Society of America*, *120*(2), 1095–1102.

Nelson, T., Boots, B., & Wulder, M. A. (2006a). Large-area mountain pine beetle infestations: Spatial data representation and accuracy. *Forestry Chronicle*, *82*(2), 243–252.

Nelson, T., Boots, B., White, K. J., & Smith, A. C. (2006b). The impact of treatment on mountain pine beetle infestation rates. *BC Journal of treatment on mountain pine beetle infestation rates*, *7*(2), 20–36.

Radeloff, V. C., Mladenoff, D. J., & Boyce, M. S. (1999). Detecting jack pine budworm defoliation using spectral mixture analysis: Separating effects from determinants. *Remote Sensing of Environment*, *69*(2), 156–169.

Roder, A., Hill, J., Duguy, B., Alloza, J. A., & Vallejo, R. (2007). Using long time series of Landsat data to monitor fire events and post-fire dynamics and identify driving factors. A case study in the Ayora region (eastern Spain). *Remote Sensing of Environment*, *112*(1), 259–273.

Rogan, J., & Miller, J. (2007). *Integrating GIS and remotely sensed data for mapping forest disturbance and change.* Boca Raton: CRC Press.

Royle, D. D., & Lathrop, R. G. (1997). Monitoring hemlock forest health in New Jersey using Landsat TM data and change detection techniques. *Forest Science*, *42*(3), 327–335.

Schroeder, T. A., Cohen, W. B., Song, C. H., Canty, M. J., & Yang, Z. Q. (2006). Radiometric correction of multi-temporal Landsat data for characterization of early successional forest patterns in western Oregon. *Remote Sensing of Environment*, *103*(1), 16–26.

Schroeder, T. A., Cohen, W. B., & Yang, Z. Q. (2007). Patterns of forest regrowth following clearcutting in western Oregon as determined from a Landsat time-series. *Forest Ecology and Management*, *243*(2–3), 259–273.

Schwalm, C. R., Black, T. A., Arniro, B. D., Arain, M. A., Barr, A. G., Bourque, C. P. A., Dunn, A. L., Flanagan, L. B., Giasson, M. A., Lafleur, P. M., Margolis, H. A., McCaughey, J. H., Orchansky, A. L., & Wofsy, S. C. (2006). Photosynthetic light use efficiency of three biomes across an east–west continental-scale transect in Canada. *Agricultural and Forest Meteorology*, *140*(1–4), 269–286.

Sinclair, T. R., Hoffer, R. M., & Schreibe, Mm. (1971). Reflectance and internal structure of leaves from several crops during a growing season. *Agronomy Journal*, *63*(6), 864–&.

Skakun, R. S., Wulder, M. A., & Franklin, S. E. (2003). Sensitivity of the thematic mapper enhanced wetness difference index to detect mountain pine beetle red-attack damage. *Remote Sensing of Environment*, *86*(4), 433–443.

Westfall, J. (2007). *2006 Summary of forest health conditions in British Columbia. B.C. Ministry of Forests, Forest Practices Branch, Victoria, B.C.*

White, J. C., Coops, N. C., Hilker, T., Wulder, M. A., & Carroll, A. L. (2007). Detecting mountain pine beetle red attack damage with EO-1 hyperion moisture indices. *International Journal of Remote Sensing*, *28*(10), 2111–2121.

Wilson, E. H., & Sader, S. A. (2002). Detection of forest harvest type using multiple dates of Landsat TM imagery. *Remote Sensing of Environment*, *80*(3), 385–396.

Wulder, M. A., White, J. C., Coops, N. C., Han, T., & Alvarez, M. F. (2005a). A protocol for detecting and mapping mountain pine beetle damage from a time-series of Landsat TM or ETM+ data. *Report prepared for the British Columbia Ministry of Forests and Range. In (p. 70): Natural Resources Canada* : Canadian Forest Service.

Wulder, M. A., Skakun, R. S., Dymond, C. C., Kurz, W. A., & White, J. C. (2005b). Characterization of the diminishing accuracy in detecting forest insect damage over time. *Canadian Journal of Remote Sensing*, *31*(6), 421–431.

Wulder, M. A., Dymond, C. C., White, J. C., Leckie, D. G., & Carroll, A. L. (2006a). Surveying mountain pine beetle damage of forests: A review of remote sensing opportunities. *Forest Ecology and Management*, *221*(1–3), 27–41.

Wulder, M. A., White, J. C., Bentz, B., Alvarez, M. F., & Coops, N. C. (2006b). Estimating the probability of mountain pine beetle red-attack damage. *Remote Sensing of Environment*, *101*(2), 150–166.

Wulder, M. A., White, J. C., Grills, D., Nelson, T., Coops, N. C., & Ebata, T. (In review). Aerial overview survey of the mountain pine beetle epidemic in British Columbia: Communication of impacts. BC Journal of Ecosystems and Management.

Zhou, Q., Li, B., & Kurban, A. (2008). Trajectory analysis of land cover change in arid environment of China. *International Journal of Remote Sensing*, *29*(4), 1093–1107.